THE JOURNAL OF PHYSICAL CHEMISTRY C

Article

pubs.acs.org/JPCC

Insights into the Preference of CO_2 Formation from HCOOH Decomposition on Pd Surface: A Theoretical Study

Riguang Zhang, Hongyan Liu, Baojun Wang,* and Lixia Ling

Key Laboratory of Coal Science and Technology of Ministry of Education and Shanxi Province, Taiyuan University of Technology, Taiyuan 030024, Shanxi, People's Republic of China

ABSTRACT: The mechanism of HCOOH decomposition on Pd(111) surface leading to the formation of CO_2 and CO has been systematically investigated to identify the preference of CO_2 or CO as the dominant product. Here, we present the main results obtained from periodic, self-consistent density functional theory calculations. Four possible pathways of HCOOH decomposition, initiated by the activation of the O−H, C−H, and C−O bonds of HCOOH, as well as the activation of simultaneous C−H and C−O bonds of HCOOH, have been proposed and discussed. Then, the effects of coadsorbed H_2O and its coverage on the decomposition of HCOOH have been also considered. Our results show that CO_2 is preferentially formed as the dominant product of HCOOH decomposition on Pd(111) surface via a dual-path mechanism, which involves both the carboxyl (*trans*-COOH) and formate (*bi*-HCOO) intermediates, along with alternative bond-breaking possible steps in those intermediates. The dehydrogenation of HCOOH on Pd surface is a vital process for CO_2 formation. Further, the coadsorbed H_2O and its coverage play an important role in the decomposition of HCOOH, and the preferred catalytic pathway of CO_2 formation is qualitatively dependent on surface H_2O coverage. Therefore, our results would at the microscopic level provide insights into the mechanism, energetics, and possible reactive intermediates of HCOOH decomposition regarding the preference of CO_2 formation as the dominant product for the catalytic reactions involving HCOOH and for a direct HCOOH fuel cell on Pd system.

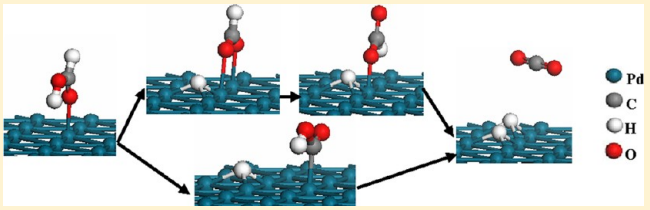

1. INTRODUCTION

The demand for power sources with superior performance has increased as a result of the rapid growth of the portable electronics market. There is a great potential for microfuel cells to deliver more energy per volume and weight than conventional batteries.[1] Up to now, the direct formic acid fuel cell (DFAFC) appears to be an attractive candidate for meeting increasing power density demands due to the advantages of high electromotive force, limited fuel crossover, and high practical power densities at low temperature. As a result, DFAFC has became a very promising power source.[2−4]

Nowadays, Pt-based and Pd-based catalysts are commonly used in DFAFC development.[5] However, Pd-based catalysts possess lower cost and higher activity than Pt-based ones for both DFAFC[2−4] and formic acid (HCOOH) decomposition,[5−11] for example, under identical conditions, the power density for Pd-based catalyst is reported to be almost 2−3 times more than that of the Pt or Pt-based alloys catalysts;[4,12,13] meanwhile, on Pt surfaces, CO poisoning due to the dehydration of HCOOH on at least two or more contiguous Pt atoms hinders the direct dehydrogenation oxidation of HCOOH,[9] as a result, the use of Pd is becoming more prevalent for practical hydrogen energy utilization. On the other hand, for the mechanism of HCOOH decomposition, the most commonly accepted mechanism is the so-called "dual pathways",[14−16] one is the pathway of dehydrogenation, the other is that of dehydration. The former may proceed via either HCOOH = CO_2 + H_2 or HCOOH = CO_2 + $2H^+$ + $2e^-$. The latter pathway leads to CO, i.e., HCOOH = CO_{ad} + H_2O. The CO adsorbed (CO_{ad}) on electrode can be oxidized only at higher potentials, contributing largely to the suppressed dehydrogenation.[17] Therefore, for DFAFC, dehydrogenation is the desired reaction pathway in order to enhance overall cell efficiency and avoid CO poisoning of the catalyst. The dehydrogenation pathway is highly desired in designing new catalysts for the best utilization of chemical energy stored in HCOOH.[10]

It is believed that the reaction pathway when using the Pd catalyst proceeds via the dehydrogenation pathway to yield CO_2 rather than that via the dehydration pathway to form CO when using Pt catalysts.[4,10,18] Meanwhile, the identity of the reactive intermediate in reaction is particularly controversial. Wilhelm and co-workers initially believed that either COH or CHO would be the reactive intermediate,[19] while others have long assumed it is COOH.[20,21] Afterward, ATR-SEIRAS studies by Osawa et al. indicated that HCOO is the reactive intermediate and that oxidation of HCOO to CO_2 is rate-determining.[22−24] Furthermore, Gao et al.[18] have indicated that HCOOH decomposition on Pt catalyst proceeds via a multipath mechanism (involving both the adsorbed HCOOH and HCOO intermediates), a result succinctly rationalizing conflicting experimental observations. Recently, the exper-

Received: December 10, 2011
Revised: October 2, 2012
Published: October 4, 2012

   dx.doi.org/10.1021/jp211900z | *J. Phys. Chem. C* 2012, 116, 22266−22280

imental studies about the decomposition of HCOOH to hydrogen production on Pd surfaces have been probed by *in situ* high-sensitivity ATR-SEIRAS,[10] which suggest that the dehydrogenation of HCOOH on Pd surface is a vital process, and CO_2 is observed as the dominant product. Although this experimental study[10] has revealed the macroscopic behavior that CO_2 is formed as the dominant product in HCOOH decomposition, unluckily, the microscopic underlying mechanisms and possible reactive intermediates of HCOOH decomposition on Pd surface regarding the preference of CO_2 as the final product remains unclear.

Nowadays, experimental information is not always sufficient and accompanying theoretical calculations can be helpful to clarify some questions. Computational chemistry methodologies have been used as a powerful tool to study the mechanism and kinetics of several typical reactions.[25−33] By means of theoretical calculation, a detailed investigation of HCOOH decomposition on Pd system at the molecular level will help us better understand the underlying mechanisms of the reactions, an atomic-scale understanding of the reaction mechanism would facilitate the design of improved catalysts. Unfortunately, to the best of our knowledge, few theoretical studies are carried out to systematically investigate the mechanism of HCOOH decomposition on Pd system.

The aim of this study is to analyze the possible reaction pathways of HCOOH decomposition occurring on the monometallic surface of Pd by carrying out periodic density functional theory slab model calculations. A large number of unique reaction pathways involving subtly different reaction intermediates and transition states are explicitly obtained, which would provide a better understanding at the molecular level the catalytic reactivity of the Pd catalyst toward the HCOOH decomposition process, as well as the possible reactive intermediates. Further, the results of this effort are expected to qualify the reaction energies and activation barriers of elementary steps involving in the reaction pathways. In addition, our results would provide insight into the energetics of HCOOH decomposition regarding the preference of CO_2 as the final product in comparison with reported experimental studies carried out in fuel cells.

2. COMPUTATIONAL DETAILS

2.1. Surface Model. In the surface calculation, the most stable face-center-cubic (111) surface of close-packed Pd metal, fcc(111), has been employed to investigate the catalytic behavior of HCOOH decomposition. Although surface orientations, such as (111), (110), or (100), could affect the energies in catalytic reactions and the electronic structures of catalysts, they might change the catalytic behaviors similarly and have limited influence in the catalytic trends on these metals with the same crystal structures.[30,34−37] The Pd(111) surface is cleaved from the experimental fcc crystal structure of lattice constant 3.89 Å, and is modeled using a three atomic layers $p(3 \times 3)$ super cell with nine atoms at each layer; this corresponds to a 1/9 monolayer (ML) coverage. A 10 Å vacuum slab is employed to separate the periodically repeated slabs. The bottom two layers are constrained at the bulk position in order to mimic the presence of a larger number of layers in real metal particles, whereas the upper layer together with the adsorbed species involved in HCOOH decomposition are allowed to relax. As shown in Figure 1, there are four different adsorption sites on Pd(111) surface: top, bridge, hcp, and fcc, within which the adsorption and dissociation of HCOOH occurs.

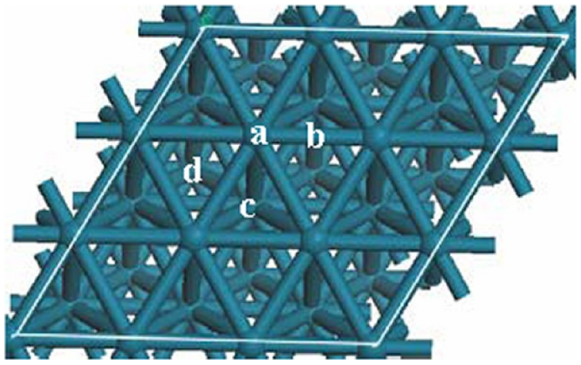

Figure 1. Top view of Pd(111)-(3 × 3) surface: (a) top site, (b) bridge site, (c) hexagonal-close-packed (hcp) site, and (d) face-centered cubic (fcc) site.

2.2. Calculation Method. All calculations are carried out in the framework of DFT using the Dmol^3 program package in Materials Studio 4.4,[38,39] where the generalized gradient approximation (GGA) corrected the exchange-correlation functional proposed by Perdew−Wang (PW91)[40] is chosen together with the doubled numerical basis set plus polarization basis sets (DNP).[41] The inner electrons of Pd atom are kept frozen and replaced by an effective core potential (ECP),[42,43] and other atoms are treated with an all−electron basis set. For the geometry optimization, the forces imposed on each atom are converged to be less than 0.0004 Ha/Å and the total energy converged to be less than 2.0×10^{-5} Ha. Brillouin-zone integrations have been performed using $3 \times 3 \times 1$ k-point grid. In order to determine accurate activation barriers of the reaction, we chose Complete LST/QST approach to search for transition states of the reactions.[44] In addition, frequency analysis has been used to validate the transition state, and TS confirmation is performed on every transition state to confirm that they lead to the desired reactants and products.

For a reaction such as AB → A + B on a Pd surface, the reaction energy (ΔH) and activation barrier (E_a) are calculated on the basis of the following formulas:

$$\Delta H = E_{(A+B)/Pd} - E_{AB/Pd}$$

$$E_a = E_{TS/Pd} - E_{AB/Pd}$$

Here $E_{(A+B)/Pd}$ is the total energy for the coadsorbed A and B on Pd surface, and $E_{TS/Pd}$ is the total energy of transition state on Pd surface. $E_{AB/Pd}$ is the total energy of adsorbate AB−Pd system in the equilibrium state.

The adsorption energy, E_{ads}, is defined as follows:

$$E_{ads} = E_{Pd} + E_{adsorbate} - E_{adsorbate/Pd}$$

Here E_{Pd} is the energy of clean Pd slab, $E_{adsorbate}$ is the energy of free adsorbate, and $E_{adsorbate/Pd}$ is the total energy of adsorbate−Pd system in the equilibrium state. With this definition, more positive values reflect the strong interaction of adsorbed species with Pd surface atoms.

2.3. Evaluation of the Method and Model. To investigate the reliability of the selected method and model, we first calculate the geometrical parameters of free HCOOH in gas phase, the O−C═O angle is 125.1 (124.0)°, and the bond lengths are 1.104 (1.097) Å for C−H, 1.356 (1.343) Å for

dx.doi.org/10.1021/jp211900z | J. Phys. Chem. C 2012, 116, 22266−22280

C−O, 1.209 (1.202) Å for C═O double bond, and 0.980 (0.972) Å for O−H. Our calculated results are in agreement with experimental values displayed in the parentheses.[45,46]

Then, to confirm the sufficiency of the chosen model (super cell of 3 × 3 and 3-layer Pd), we further compare the adsorption configuration and energy of HCOOH in the "vertical top" mode at the top site with those calculated on a larger $p(4 \times 4)$ model, the discrepancy is negligible. We also test a four-layer model using a $p(3 \times 3)$ super cell with 5 × 5 × 1 k-point grid (top two layers with adsorbates are relaxed and bottom two layers are fixed to their buck positions); the calculated adsorption energy of HCOOH is 67.6 (59.3) kJ·mol^{-1}, and the calculated activation barrier and reaction energy of O−H bond cleavage for HCOOH is 101.5 (96.5) and 5.5 (2.6) kJ·mol^{-1}. These are close to the values obtained by using a three-layer model with 3 × 3 × 1 k-point grid (see the values in parentheses, which will be obtained in below section). Therefore, considering the efficiency of calculation, the 3-layer model is suitable for our calculated systems. In addition, the 3-layer model has been used previously in the calculations of reactions on metal surface, which has shown to be effective and convincing.[46] According to above evaluations, we are confident in the ability of the chosen method and model to describe the features of the potential energy surface of HCOOH decomposition.

3. RESULTS AND DISCUSSION

In this section, we first present the proposed reaction network of HCOOH decomposition. Then, we discuss the adsorption energies and structures of the important intermediates involved in HCOOH decomposition on Pd(111) surface, and compare these results with previously reported theoretical and experimental observations. Next, we describe the transition states associated with the various elementary steps in the reaction network of HCOOH decomposition. Finally, we discuss the overall potential energy surface for this network.

3.1. Reaction Network of HCOOH Decomposition. The decomposition of HCOOH begins with the adsorption of HCOOH from the gas phase onto Pd(111) surface. The adsorbed HCOOH can then decompose via a series of sequential steps to produce various intermediates. The first decomposition step may involve the activation of the C−H, O−H and C−O bonds of HCOOH, as well as the activation of simultaneous C−H and C−O bonds of HCOOH to initiate the catalytic cycle. As a result, four possible reaction pathways for HCOOH decomposition on Pd(111) surface have been proposed, and can be summarized as Scheme 1 describes. We can see that path 1 is the pathway of HCOOH decomposition starting with O−H scission; path 2 is the pathway of C−H scission; path 3 is the pathway of C−O scission; path 4 is the pathway of simultaneous C−H and C−O bonds scission.

Scheme 1. Proposed Reaction Mechanism of HCOOH Decomposition on Pd(111) Surface

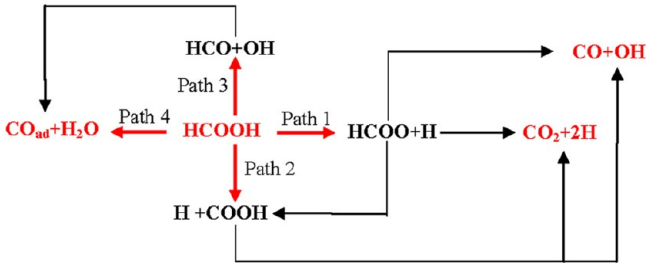

3.2. Structures and Energies of Adsorbed Species on Pd(111) Surface. *Formic Acid (HCOOH).* Two isomers of HCOOH, *trans*-HCOOH and *cis*-HCOOH, have been considered, our calculated results first show that the free *trans*-HCOOH in gas phase is more stable than that of *cis*−HCOOH. Then, two initial adsorption modes of HCOOH, "vertical top" and "parallel bridge", are investigated. For *trans*-HCOOH, the initial "vertical top" mode, the O atom of the carbonyl binds with the top Pd atom, is shown in Figure 2a. The initial "parallel bridge" mode, both C and O atoms of the carbonyl bind with two neighbor top Pd atoms on the surface is presented in Figure 2(b). The optimized configuration of "vertical top" mode is shown in Figure 2(c), which has an adsorption energy of 59.3 kJ·mol^{-1}, forming a Pd−O bond of 2.27 Å. The optimized configuration of "parallel bridge" mode (see Figure 2d) is analogous to that of "vertical top", however, HCOOH goes far away the Pd surface with a Pd−O and Pd−H distance of 2.50 and 3.02 Å, respectively, which has only an adsorption energy of 49.3 kJ·mol^{-1}. In the same way, for *cis*-HCOOH, the interaction of *cis*-HCOOH on Pd(111) surface is weaker than that of *trans*-HCOOH (39.1 vs 59.3 kJ·mol^{-1}), and *cis*-HCOOH also goes far away the surface, as shown in Figure 2e. The key geometrical parameters for *trans*-HCOOH and *cis*-HCOOH adsorbed on surface are listed in Table 1.

Therefore, the stable configuration of the optimized "vertical top" mode for *trans*-HCOOH is employed as the initial state (IS) of HCOOH decomposition on Pd(111) surface, which is denoted as **R(HCOOH)** in this study. In **R(HCOOH)**, HCOOH binds with its carbonyl oxygen to an atop site and its OH group pointing down toward another adjacent atop site, as shown in Figure 2c, which is consistent with the results of HCOOH adsorbed on Pt(111) surface obtained by Jacob et al.[18]

In the following section, we present a detailed investigation about the adsorption properties of intermediates and products for HCOOH decomposition on Pd(111) surface at the surface coverage of 1/9 ML. The most stable adsorption configurations of these adsorbed species are shown in Figure 3, and Table 1 lists some key geometrical parameters for these species.

Formate (HCOO). There are two different adsorption forms for HCOO species, monodentate and bidentate. In monodentate form, only one oxygen atom bound to the Pd atom. In bidentate formate, both oxygen atoms bound to two top Pd atoms. Our calculated results show that HCOO species in monodentate form (*mono*-HCOO) has only one stable adsorption configuration with an adsorption energy of 196.4 kJ·mol^{-1}, which adsorbed at the top site forming a Pd−O bond of 2.10 Å, as shown in Figure 3a. On the other hand, HCOO species in bidentate form adsorbed at the bridge site (*bi*-HCOO) is the most stable structure with an adsorption energy of 260.3 kJ·mol^{-1}, as presented in Figure 3b. Two Pd−O bond lengths are 2.14 and 2.14 Å, respectively. *mono*-HCOO is less stable than *bi*-HCOO. Our results are in agreement with the trend previously observed on Pd(111) surface[46] and Cu(111) surface.[47]

Formate (COOH). There are two isomers, *trans*-COOH and *cis*-COOH. Four different adsorption sites are considered, the calculated results show that *trans*-COOH adsorbed at the top site is the most stable configuration with Pd−C bond length of 1.97 Å, as presented in Figure 3c. The adsorption energy is 247.9 kJ·mol^{-1}. *cis*-COOH adsorbed at the top site is the most

dx.doi.org/10.1021/jp211900z | J. Phys. Chem. C 2012, 116, 22266−22280

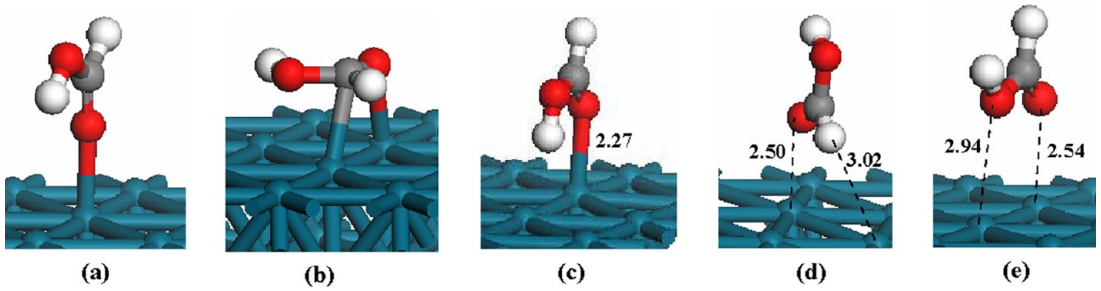

Figure 2. Initial and optimized adsorption structures of *trans*-HCOOH with (a) IS in vertical top, (b) IS in parallel bridge, (c) OS in vertical top, (d) OS in parallel bridge, and *cis*-HCOOH with (e) OS in vertical top on Pd(111) surface. IS, initial structure; OS, optimized structure. The C, O, H, and Pd atoms are shown in the gray, red, white, and dark-blue colors, respectively.

Table 1. Adsorption Sites, Adsorption Energies (kJ·mol^{-1}), and Structural Parameters (Å and deg) of the Most Stable Adsorption Structures for Adsorbed Species Involved in HCOOH Decomposition on the Pd(111) Surface

species	sites	configuration[a]	E_{ads}	$d_{C/H-Pd}$	d_{O-Pd}	$d_{C/H-O}$	d_{C-H}
trans-HCOOH	top	η^1-O	59.3	2.16	2.27	1.32, 1.23, 1.02	1.11
cis-HCOOH	top	above surface	39.1		2.94, 2.54	1.35, 1.21, 0.98	1.11
mono-HCOO	top	η^1-O	196.4	1.89	2.10	1.29, 1.21	1.20
bi-HCOO	bridge	η^1-O−η^1-O	260.3		2.14, 2.14	1.27, 1.27	1.11
trans-COOH	top	η^1-C	247.9	1.97		1.23, 1.34, 0.98	
cis-COOH	top	η^1-C	232.1	1.97		1.22, 1.35, 0.98	
HCO	fcc	η^2-C−η^1-O	241.3	2.08, 2.09	2.21	1.26	1.11
OH	fcc	η^2-O	253.0		2.16, 2.16	0.98	
H_2O	top	above surface	49.3			0.97, 0.98	
CO	fcc	η^3−C	197.9	2.08, 2.09, 2.09		1.19	
H	fcc	η^3−H	280.7	1.81			
CO_2	bridge	above surface	17.6		3.26, 3.29	1.18, 1.18	

[a] η^m−C−η^n−O denotes the adsorbate adsorbs via the C and O atoms with *m* and *n* surface metal atoms, respectively.

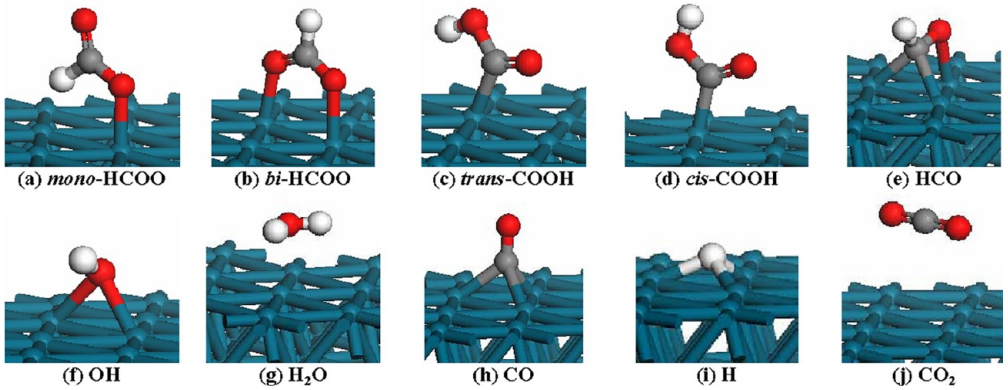

Figure 3. The most stable adsorption structures of intermediates involved in HCOOH decomposition on Pd(111) surface. See Figure 2 for color coding.

stable structure with an adsorption energy of 232.1 kJ·mol^{-1}, as shown in Figure 3d, only one carbon atom is bound to Pd atom, and the Pd−C bond length is 1.97 Å. In addition, the free *trans*-COOH in gas phase is found to be more stable than the free *cis*-COOH in gas phase, the interaction of *trans*-COOH with Pd(111) surface is also stronger than that of *cis*-COOH (247.9 vs. 232.1 kJ·mol^{-1}). Therefore, the stable configuration of *trans*-COOH adsorbed on Pd(111) surface is chosen as the final state (FS) of HCOOH decomposition initiated by C−H bond cleavage.

Formyl (HCO). HCO species bind to Pd(111) surface either via the carbon atom in η^1-C configuration, where HCO moiety forms a V-shape structure with the C atom close to the surface or simultaneously via both C and O atoms in η^2-C−η^1-O configuration, where the molecular plane is perpendicular to the surface and the C−O bond is nearly parallel to the surface. According to our calculations, HCO exhibits a clear preference at the fcc site with η^2-C−η^1-O configuration on Pd(111) surface, as shown in Figure 3e; the stable configuration has an adsorption energy of 241.3 kJ·mol^{-1}.

Hydroxyl (OH). The optimized geometry for OH is found to bind in a perpendicular orientation toward the surface with O binding to the Pd(111) surface. We find that OH prefers binding to the bridge site with an adsorption energy of 253.0 kJ·mol^{-1}. In addition, the initial structure of OH adsorbed at the top site is converted to bridge site. OH adsorbed at the hcp

dx.doi.org/10.1021/jp211900z | J. Phys. Chem. C 2012, 116, 22266−22280

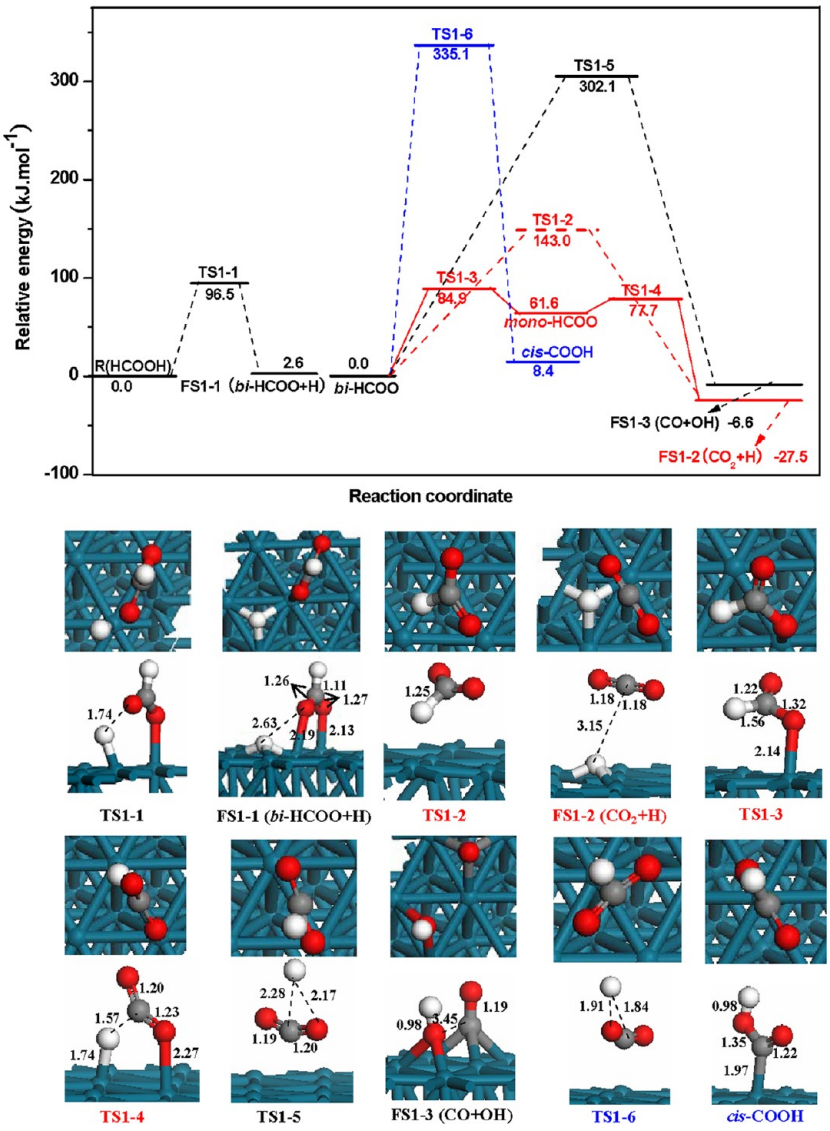

Figure 4. Potential energy profiles for HCOOH decomposition initiated by the O−H bond cleavage to CO_2 (red line) and to CO (black line), as well as to *cis*-COOH (blue line) on Pd(111) surface in together with the structures of the intermediates, transition states and products. TS, transition state; FS, final state. Bond lengths are in Å. See Figure 2 for color coding.

and fcc sites have the adsorption energies of 232.5 and 246.3 kJ·mol^{-1}, respectively. The most stable configuration for OH binding to the bridge site is with its H atom tilted, as revealed in Figure 3f. The additional stability is due to the interaction between H and the surface for the titled structure, similar to the case at the top site of Cu(111) surface.[48]

Water (H_2O). According to our calculations, H_2O interacts weakly with the Pd(111) surface. In the optimized configurations at all adsorption sites, H_2O is far away from the surface; the H−O bond lengths and the angle of O−C−O are closed to those in the gas phase H_2O molecule. The most stable configuration for H_2O is that H_2O molecular plane is parallel to the surface, as presented in Figure 3g, which has an adsorption energy of 49.3 kJ·mol^{-1}.

Carbon Monoxide (CO). Scanning tunneling microscopy indicates that CO on Pd(111) surface occupies hollow sites.[49] Optimized geometrical structures show that CO adsorbed with a perpendicular orientation toward the surface and with C (carbon atom) bound to the metallic surface. Our calculations indicate that there is a preference for CO to bind to fcc sites on the Pd(111) surface with the adsorption energy of 197.9 kJ·mol^{-1}, as shown in Figure 3h, which is in good agreement with previously reported results for Pd(111) surface at the most favorable fcc sites.[50,51]

Atomic Hydrogen (H). Low-energy electron diffraction study shows that H atoms reside at fcc 3-fold hollow sites on Pd(111) surface.[52] Many theoretical studies on Pd surfaces corroborated that H atoms prefer high-coordination hollow sites, but there is no agreement concerning the most favorable site.[53,54] We found the different adsorption energies of atomic H, 280.7 and 275.7 kJ·mol^{-1}, at the fcc and hcp sites of Pd(111) surface, respectively; these values are somewhat lower than the BP-GGA result of the cluster model H_8/Pd_{79}, 311 kJ·mol^{-1},[53] but close to the experimental value, 259.0 kJ·mol^{-1}.[55] Thus, atomic H adsorbed at the fcc site is the stable configuration, as displayed in Figure 3i. However, such a small range of energy values between fcc and hcp sites indicates a rather flat PES of H on Pd(111) surface, implying significant mobility of adsorbed H. H adsorbates on Pd may show a propensity to diffuse to subsurface positions at high coverage, yet at low coverage as

dx.doi.org/10.1021/jp211900z | J. Phys. Chem. C 2012, 116, 22266−22280

considered here, atomic H species in subsurface positions appear to be thermodynamically disfavored.[53]

Carbon Dioxide (CO_2). We observe that CO_2 interacts weakly with the Pd(111) surface. For all adsorption sites, CO_2 is far away from the surface in the optimized configurations, and the C−O bond lengths and the angle of O−C−O are close to those in the gas phase CO_2 molecule. This is in agreement with experimental report that CO_2 prefers to remain as a free species rather than adsorbed on the metallic surfaces.[56] The relatively stable configuration with an adsorption energy of 17.6 kJ·mol^{-1} is presented in Figure 3j, in which CO_2 lies above the Pd−Pd bridge.

3.3. Thermodynamics and Kinetics of the HCOOH Decomposition Reaction Network. Having established the basic energetic and geometric features of adsorbates on Pd(111) surface, we turn to a description of the energetics of the complex reaction networks associated with HCOOH decomposition on Pd(111) surface in this section. For simplicity, we choose the adsorption of the involved intermediates at the most stable site as the initial state (IS) of reaction, and the corresponding final state (FS) of reaction is taken to be the coadsorption of the product species at their most stable sites. Reaction energy and activation barrier of every elementary reaction have been obtained.

3.3.1. HCOOH Decomposition through O−H Bond Activation. The pathway for HCOOH decomposition is initiated by the O−H bond activation of R(HCOOH). Using R(HCOOH) as the initial state, as shown in Figure 2c, we study the formation of CO_2 and CO in path 1, as shown in Scheme 1. The potential energy profile following the pathway from R(HCOOH) to CO_2 and CO is presented in Figure 4. The structures with key parameters of all the intermediates, transition states and product involved in this pathway are shown together with the potential energy profile.

(A). CO_2 Formation. Starting from R(HCOOH), the O−H bond cleavage of HCOOH can form the coadsorbed formate and hydrogen (FS1−1) through a transition state TS1−1. In FS1−1, *bi*-HCOO + H, H is the H atom of OH group in HCOOH and located at the fcc site, *bi*-HCOO species in a bidentate form binds the substrate through two O−Pd (2.19 and 2.13 Å) bonds, as shown in Figure 4. As already mentioned in section 3.2, they are the most stable configuration of H atom and HCOO species on Pd(111) surface, respectively. Two C−O bonds are 1.26 and 1.27 Å, respectively, and the O_a−C−O_b angle is 129.9°. These structural properties are similar to those observed in HCOO adsorption on Cu surface.[57−60] In this step, the main component of the reaction coordinate is elongation of the O−H bond; this bond is extended to 1.74 Å in TS1−1, 2.63 Å in FS1−1 from 1.02 Å in their initial *trans*-HCOOH equilibrium bond length. The activation barrier for this elementary reaction is 96.5 kJ·mol^{-1}, and the reaction is found to be slightly endothermic by 2.6 kJ·mol^{-1}.

Then, *bi*-HCOO species is selected as the initial state, which can react directly to form FS1−2, CO_2 + H, H is located at the fcc site, CO_2 molecule is far away from the surface, as already mentioned in section 3.2, they are the most stable configuration of H atom and CO_2 molecule on Pd(111) surface, respectively. In FS1−2, the O−C−O angle of CO_2 is 179.4°, and two C−O bond lengths are 1.18 Å, which are close to those in the gas phase CO_2 molecule. This step goes through a direct C−H bond cleavage of *bi*-HCOO via the transition state TS1−2. The C−H bond is elongated from 1.11 Å in *bi*-HCOO to 1.25 Å in TS1−2, and 3.15 Å in FS1−2. This elementary reaction has a high activation barrier of 143.0 kJ·mol^{-1}, and is exothermic by 27.5 kJ·mol^{-1}.

On the other hand, an alternative route to form CO_2 is possible if the bidentate *bi*-HCOO rearranges to a monodentate *mono*-HCOO. According to our calculations, *bi*-HCOO can be isomerized to *mono*-HCOO by breaking an O−Pd bond via the transition state TS1−3, this step is endothermic by 61.6 kJ·mol^{-1}, with an activation barrier of 84.9 kJ·mol^{-1}. Subsequently, *mono*-HCOO can easily break its C−H bond through a transition state TS1−4 to form FS1−2, CO_2 + H. In this step, the distances between C and H increase from 1.20 Å in *mono*-HCOO to 1.57 Å in TS1−4, and 3.15 Å in FS1−2. This step is highly exothermic by 89.1 kJ·mol^{-1}, with a small activation barrier of 16.1 kJ·mol^{-1}.

(B). CO Formation. After the initial O−H bond scission event in HCOOH leading to *bi*-HCOO species, *bi*-HCOO can occur through the transition state TS1−5 of a concerted C−H and C−O bond cleavages. In TS1−5, the O−H and C−H distances are 2.17 and 2.28 Å, respectively. This step will directly leads to the FS1−3, CO + OH, OH (0.98 Å) is located at the bridge site, CO (1.19 Å) is adsorbed at the fcc site. The distance between C atom of CO and O atom of OH group is 3.45 Å. As mentioned before, they are the most stable configurations of OH and CO species on Pd(111) surface, respectively. This step is slightly exothermic by 6.6 kJ·mol^{-1}, with a significantly high activation barrier of 302.1 kJ·mol^{-1}. In addition, an alternative route to form CO starting from *mono*-HCOO species has been also considered, our results show that this reaction first leads to the formation of CO_2 + H due to the small activation barrier of 16.1 kJ·mol^{-1}.

(C). The Isomerization of bi-HCOO Species. As with the O−H bond cleavage in HCOOH to form *bi*-HCOO species, *bi*-HCOO may be isomerized to *cis*-COOH by breaking a C−H bond via a transition state TS1−6. In this step, hydrogen is transferred from C atom to O atom, and an O−H bond is newly formed. In TS1−6, the O−H and C−H distances are 1.91 and 1.84 Å, respectively. This step is slightly endothermic by 8.4 kJ·mol^{-1}, with a highest activation barrier of 335.1 kJ·mol^{-1}.

(D). Brief Summary. Following the potential energy profile from R(HCOOH) to CO_2 and CO, as presented in Figure 4, we can see that for the formation of CO_2 with respect to *bi*-HCOO species, the highest barrier and reaction energy through a *mono*-HCOO intermediate in a red solid line are +84.9 and −27.5 kJ·mol^{-1}, respectively, whereas those for the direct formation of CO_2 in a red dash line are +143.0 and −27.5 kJ·mol^{-1}, respectively. On the other hand, for the direct formation of CO with *bi*-HCOO species, the highest barrier and reaction energy in a black solid line are +302.1 and −6.6 kJ·mol^{-1}, respectively. In addition, the highest barrier and reaction energy for the isomerization of *bi*-HCOO to *cis*-COOH in a blue line are 335.1 and 8.4 kJ·mol^{-1}, respectively.

As a result, starting from *bi*-HCOO species, we can see that the formation of CO_2 through a *mono*-HCOO intermediate becomes more favorable both kinetically and thermodynamically in comparison with other routes, which means that the dominant product of the initial O−H bond cleavage of HCOOH on Pd(111) surface is CO_2. The detailed route of CO_2 formation is carried out as follows: R(HCOOH) → *bi*-HCOO + H → *mono*-HCOO + H → CO_2 + 2H, in which the O−H bond cleavage of HCOOH is the rate-determining step with an activation barrier of 96.5 kJ·mol^{-1}.

dx.doi.org/10.1021/jp211900z | J. Phys. Chem. C 2012, 116, 22266−22280

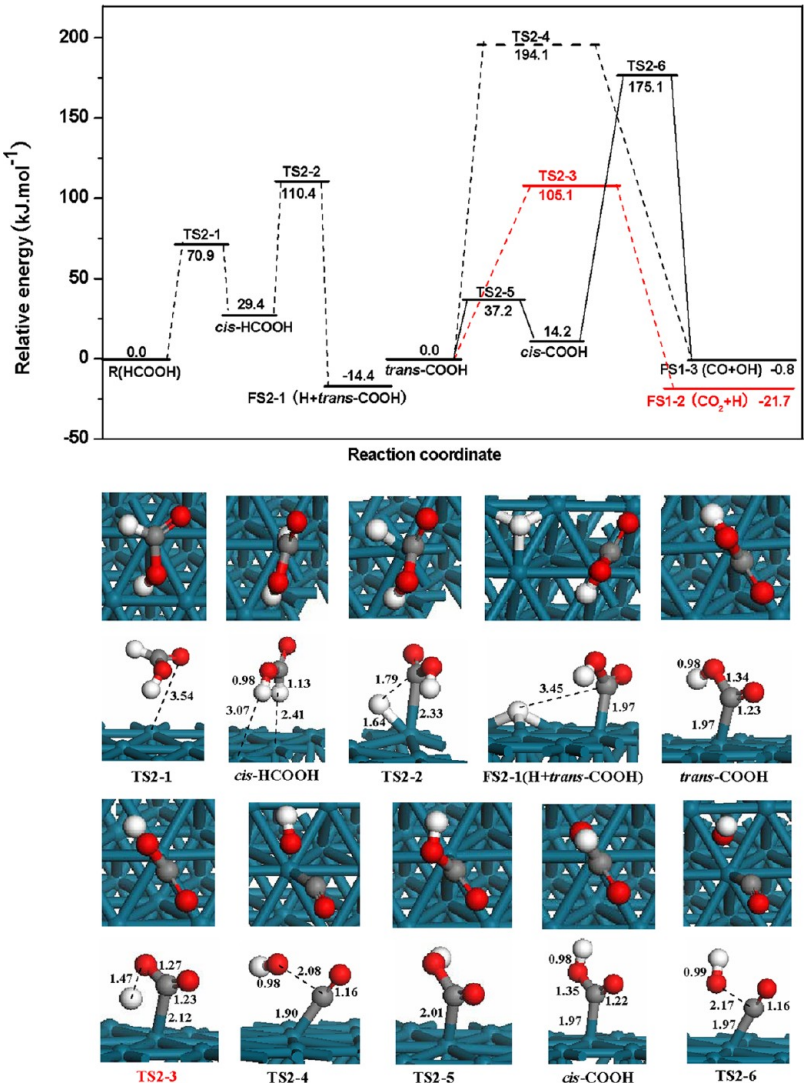

Figure 5. Potential energy profiles for HCOOH decomposition initiated by the C−H bond cleavage to CO_2 (red line) and to CO (black line) on Pd(111) surface along with the structures of the intermediates, transition states, and products: TS, transition state; FS, final state. Bond lengths are in Å. See Figure 2 for color coding.

3.3.2. HCOOH Decomposition through C−H Bond Activation. Using R(HCOOH) as the initial state, we have studied the formation of CO_2 and CO initiated through the C−H bond activation in path 2, as illustrated in Scheme 1. The potential energy profile from R(HCOOH) to CO_2 and CO is shown in Figure 5, and the corresponding structures with key parameters are also presented on the potential energy diagram.

Starting from R(HCOOH), *trans*-HCOOH species first isomerizes into an unstable *cis*-HCOOH species through a transition state TS2−1. *cis*-HCOOH species is far away from the surface with two Pd−H distances of 3.07 and 2.41 Å. The activation barrier for this elementary reaction is 70.9 kJ·mol^{-1}, and the reaction is found to be endothermic by 29.4 kJ·mol^{-1}. Subsequently, the C−H bond activation cleavage of *cis*-HCOOH can lead to the formation of formate and hydrogen intermediates (FS2−1) through a transition state TS2−2. The distances between C and H are elongated from 1.13 Å in *cis*-HCOOH to 1.79 Å in TS2−2, and 3.45 Å in FS2−1. In FS2−1, *trans*-COOH + H, H atom located at the fcc site, a more stable *trans*-COOH species is formed, which binds the substrate through a newly formed C−Pd bond (1.97 Å), as presented in Figure 5. FS2−1 is the coadsorbed configuration of the most stable configuration of H atom and *trans*-HCOO species on Pd(111) surface. This step is found to be exothermic by 43.8 kJ·mol^{-1}, with an activation barrier of 81.0 kJ·mol^{-1}.

Then, the decomposition of adsorbed *trans*-COOH may proceed along two different pathways, *trans*-COOH → CO_2 + H and *trans*-COOH → CO + OH. For the former pathway, after the O−H bond cleavage, the FS1−2, CO_2 + H, is formed through a transition state TS2−3. In TS2−3, O−H bond is extended to 1.47 Å from 0.98 Å in *trans*-COOH. The activation barrier for this elementary reaction is 105.1 kJ·mol^{-1} and the reaction is found to be slightly exothermic by 21.7 kJ·mol^{-1}. For the latter pathway, after the O−C bond activation, the dissociation of *trans*-COOH via the transition state TS2−4 can generate the FS1−3, CO + OH. The distance between C atom and O atom of OH group are elongated to 2.08 Å in TS2−4 from 1.34 Å in *trans*-COOH. The activation barrier for this elementary reaction is 194.1 kJ·mol^{-1} and the reaction is slightly exothermic by 0.8 kJ·mol^{-1}.

Further, an alternative route to form CO_2 or CO is possible if *trans*-COOH can isomerize to an unstable *cis*-HCOO species.

dx.doi.org/10.1021/jp211900z | J. Phys. Chem. C 2012, 116, 22266−22280

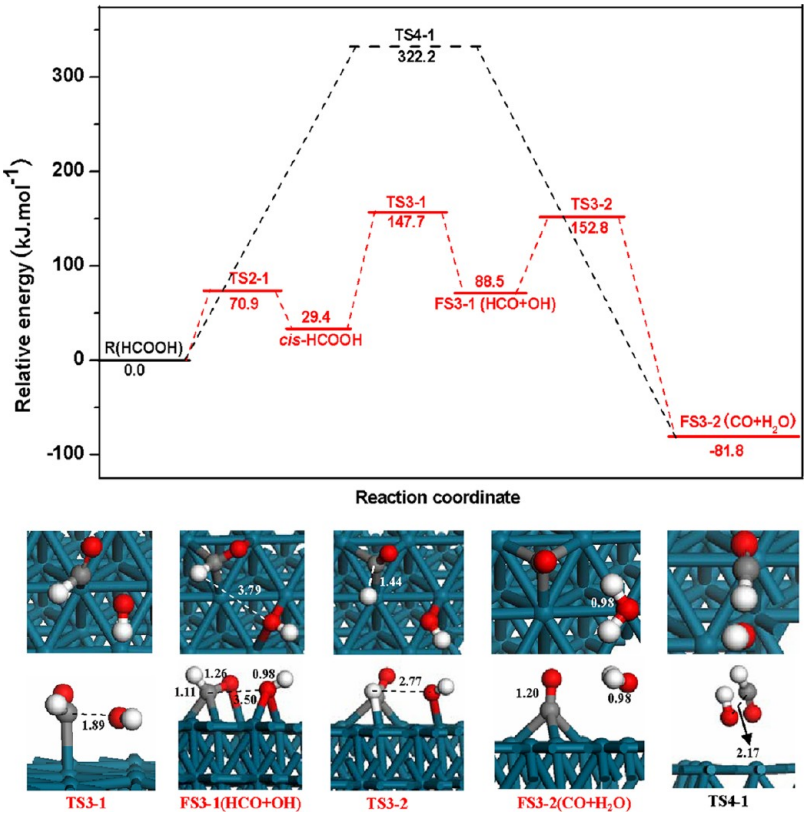

Figure 6. Potential energy profiles for HCOOH decomposition to CO initiated by the C−O bond cleavage (red line) and the simultaneous C−O and O−H bond cleavages (black line) on Pd(111) surface. The structures of the intermediates, transition states, and products involved in reaction are also shown: TS, transition state; FS, final state. Bond lengths are in Å. See Figure 2 for color coding.

According to our calculations, *trans*-COOH can be isomerized to *cis*-HCOO via the transition state TS2−5, this step is endothermic by 14.2 kJ·mol^{-1}, with a small activation barrier of 37.2 kJ·mol^{-1}. Similarly, the decomposition of *cis*-COOH may proceed along two pathways, *cis*-COOH → CO_2 + H and *cis*-COOH → CO + OH. For the former pathway, our results show that this reaction must go through an intermediate *trans*-COOH, subsequently, its O−H bond cleavage forms CO_2 + H. For the latter pathway, *cis*-COOH can break its C−O bond through a transition state TS2−6 to form FS1−3, CO + OH. The distance between C atom and O atom of OH group are elongated to 2.17 Å in TS2−6 from 1.35 Å in *cis*-COOH. The activation barrier for this elementary reaction is 160.9 kJ·mol^{-1} and the reaction is exothermic by 15.0 kJ·mol^{-1}. In addition, *In situ* IR studies by Holdcroft and Funt[61] have revealed that the formation of adsorbed CO is from the intermediate COOH.

As a result, we can see from Figure 5 that the highest barrier and reaction energy for CO_2 formation with respect to *trans*-COOH species in a red line are +105.1 and −21.7 kJ·mol^{-1}, respectively, whereas those for the direct formation of CO in a black dash line are +194.1 and −0.8 kJ·mol^{-1}, respectively; those for the indirect formation of CO through a *cis*-COOH intermediate in a black solid line are +175.1 and −0.8 kJ·mol^{-1}, respectively. Our result means that the formation of CO_2 is more preferable both kinetically and thermodynamically than CO formation, suggesting that CO_2 is the dominant product of the initial C−H bond activation of HCOOH on Pd(111) surface. The detailed reaction route of CO_2 formation is carried out as follows: R(HCOOH)→*trans*-COOH + H → CO_2 + 2H, in this route, the O−H bond cleavage of *trans*-COOH is the rate-determining step with an activation barrier of 110.4 kJ·mol^{-1}.

3.3.3. HCOOH Decomposition through C−O Bond Activation. Although the dehydrogenation mechanisms initiated by the O−H and C−H bond cleavages appear to be energetically favorable in the HCOOH decomposition process, it is nonetheless important to consider competing pathways and elementary steps on Pd(111) surface. In Figure 6, we give out the potential energy diagram for C−O bond cleavage of HCOOH itself and its dehydrogenation process using a red line in path 3; the corresponding structures with key parameters are also presented on this figure.

Starting from R(HCOOH), *trans*-HCOOH first isomerizes into an unstable *cis*-HCOOH through a transition state TS2−1. The activation barrier for this elementary reaction is 70.9 kJ·mol^{-1} and the reaction is found to be endothermic by 29.4 kJ·mol^{-1}. Subsequently, the C−O bond cleavage of HCOOH can form formyl and hydroxyl intermediates through a transition state TS3−1. In FS3−1, HCO + OH, OH adsorbed at the bridge site, HCO species binds the substrate via both C and O atoms in η^2-C−η^1-O configuration, both are the most stable configuration of OH and HCO species on Pd(111) surface, respectively. The main component of the reaction coordinate for this elementary step is the elongation of the C−O bond; this bond is extended to 1.89 Å in TS3−1, 3.50 Å in FS3−1 from 1.32 Å in the equilibrium *trans*-HCOOH. The activation barrier for this step, 118.3 kJ·mol^{-1}, is considerably larger than those for the O−H and C−H bond cleavage. This step is highly endothermic by 59.1 kJ·mol^{-1}.

Then, the C−H bond of HCO can be activated, this step goes through a hydrogen migration from C atom of HCO to O

dx.doi.org/10.1021/jp211900z | J. Phys. Chem. C 2012, 116, 22266−22280

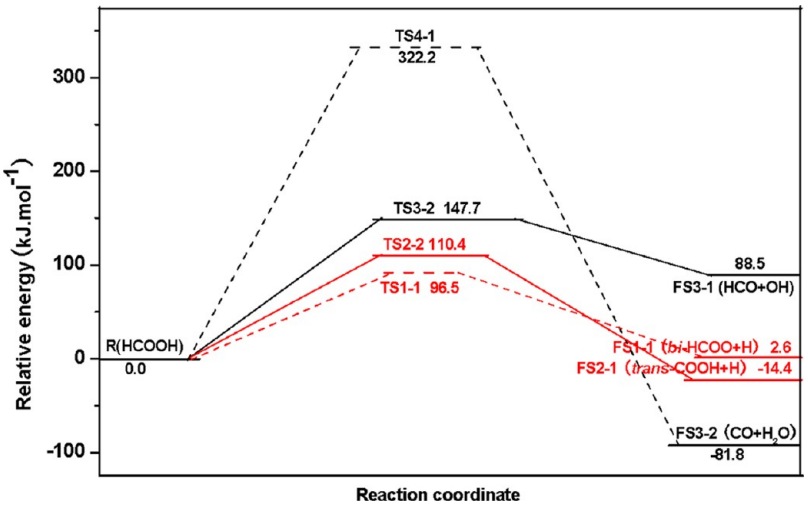

Figure 7. Schematic potential energy diagrams of the initial step for O−H (red dash line), C−H (red solid line), C−O bond (black solid line), as well as simultaneous O−H and C−H bond cleavages (black dash line) of HCOOH on Pd(111) surface, respectively. Only transition state (TS) with the highest barrier for each path is shown.

atom of OH group leading to the formation of CO adsorbed and H_2O (FS3−2) via a transition state TS3−2. In FS3−2, CO + H_2O, CO adsorbed at the fcc site, H_2O is far away the surface, and its molecular plane is parallel to the surface. As mentioned before, they are also the most stable configuration of CO and H_2O species on Pd(111) surface, respectively. In this step, the distance between O atom in OH group and H atom in HCO is shorten to 2.77 Å in TS3−2, 0.98 Å in FS3−2 from 3.79 Å in FS3−1. This step is highly exothermic by 170.3 kJ·mol^{-1}, with an activation barrier of 64.3 kJ·mol^{-1}.

3.3.4. HCOOH Decomposition through Simultaneous C−H and O−H Activation. Using R(HCOOH) as the initial state, for the simultaneous C−H and O−H bonds activation of HCOOH in Path 4, the direct pathway through the transition state TS4−1 can lead to the formation of FS3−2, CO + H_2O. Figure 6 presents the potential energy diagram using a black line. We can see that this elementary reaction has a very large activation barrier of 322.2 kJ·mol^{-1}, with the reaction exothermic by 81.8 kJ·mol^{-1}.

3.3.5. General Discussion. Figure 7 shows a simplified potential energy diagram by only including the highest barrier of the initial step for the cleavage of O−H, C−H, C−H bond of HCOOH, as well as the simultaneous O−H and C−H bonds cleavage of HCOOH on Pd(111) surface, respectively. As shown in this figure, with respect to R(HCOOH) species, the highest barrier and reaction energy of the initial step for C−O bond cleavage in a black solid line are 147.7 and 88.5 kJ·mol^{-1}, respectively, whereas, those for the simultaneous O−H and C−H bonds cleavage in a black dash line are 322.2 and −81.8 kJ·mol^{-1}, respectively. As a result, C−O bond cleavage is more favorable kinetically, whereas simultaneous O−H and C−H bonds cleavage is preferred thermodynamically. But the highest barrier of simultaneous O−H and C−H bonds cleavage is far larger than that of C−O bond cleavage, which means that simultaneous O−H and C−H bonds cleavage of HCOOH is unlikely to be favorable pathway in comparison with the C−O bond cleavage of HCOOH on Pd(111) surface.

On the other hand, the initial step for O−H bond cleavage of HCOOH, the highest barrier and reaction energy in a red dash line are 96.5 and 2.6 kJ·mol^{-1}, respectively, whereas, those for C−H bond cleavage in a red solid line are 110.4 and −14.4 kJ·mol^{-1}, respectively. Both the highest barrier and reaction energy for the O−H or C−H bond cleavage of HCOOH are lower than the corresponding values for C−O bond cleavage of HCOOH, suggesting that the O−H or C−H bond cleavage leading to *bi*-HCOO or *trans*-COOH intermediate is more favorable both kinetically and thermodynamically in comparison with C−O bond cleavage forming HCO and OH intermediates. Further, the highest barrier of C−O bond cleavage of HCOOH (147.7 kJ·mol^{-1}) is also far larger than those of C−H breaking in *bi*-HCOO intermediate (84.9 kJ·mol^{-1}) and O−H bond cleavage in *trans*-COOH intermediate (105.1 kJ·mol^{-1}), strongly implying that C−O cleavage of HCOOH is unlikely to be a major reaction pathway for HCOOH decomposition on Pd(111) surface in comparison with C−H or O−H bond cleavage of HCOOH.

In addition, the decomposition of HCOOH is analogous to that of CH_3OH, since both are initiated through C−H, O−H and C−O bond breaking. Mehmood et al.[62] have investigated CH_3OH decomposition on Pd clusters through C−H, O−H and C−O bond breaking, their results also show that C−O cleavage is impossible to be a major reaction pathway in comparison with C−H or O−H bond cleavage. Moreover, the adsorption of HCOOH and its dehydrogenation intermediates on Pd(100) surface have already been studied by Yue and Lim,[13] their studies show that the initial C−H bond cleavage is more favorable thermodynamically by 25.0 kJ·mol^{-1} than O−H bond cleavage, which is close to our values by 17.0 kJ·mol^{-1}, so they think the reaction should proceed along both of the two pathways due to little differences between the initial cleavage of O−H and C−H bond thermodynamically. However, the studies by Zhou et al.[46] indicate that for adsorbed HCOOH on Pd(111) surface, the initial O−H bond cleavage is more favorable kinetically by 10.3 kJ·mol^{-1} than C−H bond cleavage, which is in agreement with our calculated results by 13.9 kJ·mol^{-1}, so their conclusion is that dehydrogenation of HCOOH is mainly initiated by cleavage of O−H bond.

On the basis of these reported studies and our results, we think that although O−H bond cleavage of HCOOH is more favorable kinetically (13.9 kJ·mol^{-1}), whereas C−H bond cleavage of HCOOH is preferred thermodynamically (17.0 kJ·mol^{-1}) in our study, the differences between the initial

dx.doi.org/10.1021/jp211900z | J. Phys. Chem. C 2012, 116, 22266−22280

Scheme 2. Mechanistic Scheme for HCOOH Decomposition on Pd(111) Surface

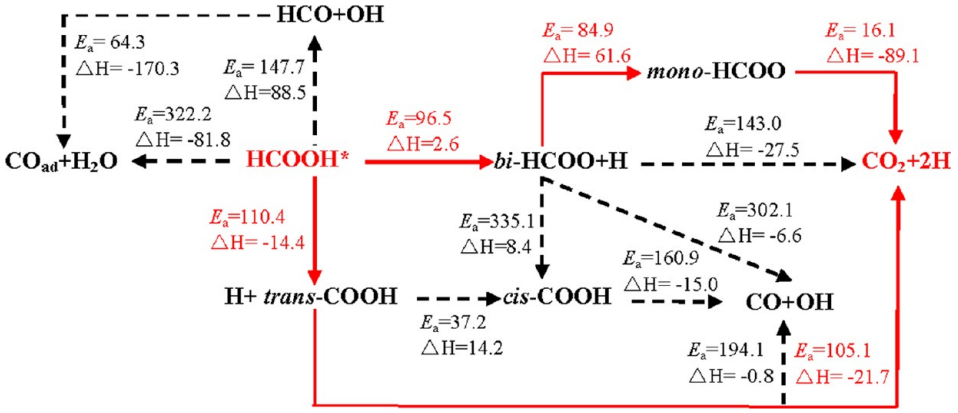

cleavage of O−H and C−H bond thermodynamically and kinetically are small. Thus, we can conclude that the reaction of HCOOH decomposition along both of the O−H and C−H bond cleavage should be a parallel pathway, namely, dehydrogenation of HCOOH is mainly initiated by the cleavage of O−H and C−H bond of HCOOH, which lead to the formation of *bi*-HCOO and *trans*-COOH intermediates, respectively. As mentioned before, starting from the *bi*-HCOO and *trans*-COOH intermediates, the formation of CO_2 is more preferable both kinetically and thermodynamically than CO formation, suggesting that CO_2 is the dominant product of the initial O−H and C−H bond cleavage of HCOOH on Pd(111) surface.

As a result, according to our calculation, mechanistic scheme for HCOOH decomposition on Pd(111) surface is illustrated in Scheme 2. As shown in this scheme, CO_2 is preferentially formed as the dominant product of HCOOH decomposition on Pd(111) surface via a dual-path mechanism along with the red arrows, which involves both the carboxyl (*trans*-COOH) and formate (*bi*-HCOO) intermediates, along with alternative bond-breaking possible steps in those intermediates. The dehydrogenation of HCOOH on Pd surface is a vital process for CO_2 formation.

3.4. The Effect of Coadsorbed H_2O and Its Coverage on the Adsorption and Decomposition. Above studies are mainly focus on the adsorption and decomposition of HCOOH in the gas phase under a low coverage of 1/9 ML to probe into the mechanism, energetics and possible reactive intermediates of HCOOH decomposition regarding the preference of CO_2 formation as the dominant product for vapor phase catalysis involving HCOOH and for direct HCOOH fuel cell on Pd system. However, in the case of the electrocatalytic oxidation of HCOOH, the effect of coadsorbed H_2O molecules on the adsorption and decomposition of HCOOH should be taken into account. As I know, H_2O molecule can affect the electrocatalytic oxidation of HCOOH, for example, the studies by Wang et al.[18] have investigated the effect of H_2O molecules on the electro-oxidation of HCOOH on Pt(111), suggesting that H_2O molecule can affect the energies and geometric structures of intermediates and transition states. As a result, to elucidate whether H_2O molecule and its coverage can effectively affect the electro-catalytic oxidation of HCOOH on Pd, we further investigate the effect of coadsorbed H_2O molecule and its coverage on the initial adsorption of HCOOH and its decomposition on Pd(111) surface in the presence of the coadsorbed single and two H_2O molecules, respectively.

3.4.1. The Effect of Coadsorbed H_2O and Its Coverage on the Initial Adsorption of HCOOH. For the effect of coadsorbed H_2O on the initial adsorption of HCOOH, as mentioned above, a single H_2O molecule within a (3×3) unit cell binds to the Pd(111) surface in the gas phase with an adsorption energy of 49.3 kJ·mol^{-1}, and a single HCOOH binds to this surface in the gas phase with an adsorption energy of 59.3 kJ·mol^{-1}, forming a Pd−O bond of 2.27 Å. In this section, the stable configuration of HCOOH adsorption in the presence of single H_2O molecule and two H_2O molecules on this surface have been presented in Figure 8. Our results show that the

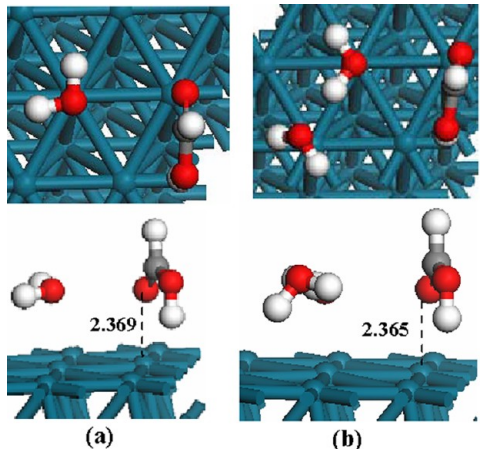

Figure 8. The side and top views of the most stable adsorption structures of HCOOH on Pd(111) surface in the presence of the coadsorbed single and two H_2O molecules: (a) single H_2O; (b) two H_2O. See Figure 2 for color coding.

adsorption energy of HCOOH in the presence of single H_2O molecule is 58.2 kJ·mol^{-1}, the distance between the O atom of the carbonyl and the top Pd atom is 2.369 Å. The adsorption energy of HCOOH in the presence of two H_2O molecules is 57.7 kJ·mol^{-1}, the distance between the O atom of the carbonyl and the top Pd atom is 2.365 Å. In these two stable configurations, the O atom of the carbonyl does not bind with the top Pd atom due to the existence of H_2O, suggesting that the coadsorbed H_2O molecule and its coverage can little reduce the adsorption ability and slightly affect adsorption configuration of HCOOH on Pd(111) surface, namely, the effect of H_2O molecule on HCOOH adsorption is negligible.

dx.doi.org/10.1021/jp211900z | J. Phys. Chem. C 2012, 116, 22266−22280

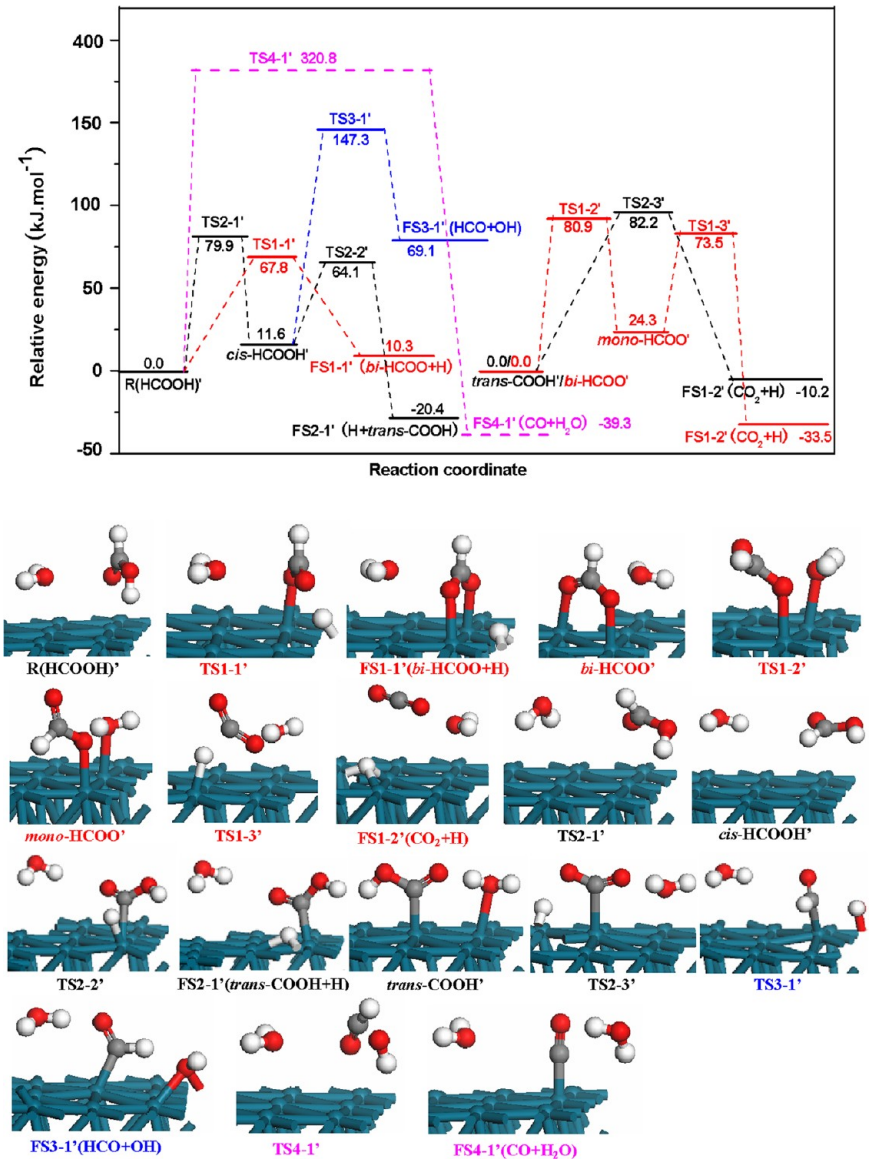

Figure 9. Potential energy profiles for HCOOH decomposition on Pd(111) surface in the presence of single adsorbed H_2O molecule, as well as the structures of the intermediates, transition states and products: TS, transition state; FS, final state. Bond lengths are in Å. See Figure 2 for color coding.

3.4.2. The Effect of Coadsorbed H_2O and Its Coverage on the Decomposition of HCOOH. For the decomposition of HCOOH in the presence of coadsorbed H_2O, the reaction potential energy profiles of HCOOH decomposition and the corresponding structures of the intermediates, transition states and products have be presented in Figures 9 and 10. The activation barrier and reaction energy of every elementary reaction involving in HCOOH decomposition are listed in Table 2.

(A). HCOOH Decomposition in the Presence of the Coadsorbed Single H_2O Molecule. When a single H_2O molecule is coadsorbed with HCOOH on Pd(111) surface, as shown in Figure 9, we can obtain the following data. ***(I) The initial O−H bond cleavage of HCOOH***: the activation barrier and reaction energy for the initial O−H bond cleavage of HCOOH are 67.8 and 10.3 kJ·mol^{-1}, respectively; for the formation of CO_2 with respect to *bi*-HCOO species, the highest barrier and reaction energy through a *mono*-HCOO intermediate are 80.9 and −33.5 kJ·mol^{-1}, respectively, the route of CO_2 formation is still carried our as follows: R(HCOOH) → *bi*-HCOO + H → *mono*-HCOO + H → CO_2 + 2H, however, the rate-determining step becomes the isomerization of *bi*-HCOO to *mono*-HCOO with the highest barrier and reaction energy of 80.9 and −33.5 kJ·mol^{-1} in comparison with that of the initial O−H bond cleavage of HCOOH in the gas phase with the highest barrier and reaction energy of 96.5 and 2.6 kJ·mol^{-1}, respectively. ***(II) The initial C−H bond cleavage of HCOOH***: the activation barrier and reaction energy for the initial C−H bond cleavage of HCOOH are 79.9 and −20.4 kJ·mol^{-1}, respectively; for the formation of CO_2 with respect to *trans*-COOH species, the highest barrier and reaction energy are 82.2 and −10.2 kJ·mol^{-1}, respectively. The reaction route of R(HCOOH)→ *trans*-COOH + H → CO_2 + 2H is responsible for CO_2 formation, however, both the initial C−H bond cleavage of HCOOH and the O−H bond cleavage of *trans*-COOH become the common rate-determining step in comparison with that of the initial C−H bond cleavage of HCOOH in the gas phase with the highest barrier and reaction

dx.doi.org/10.1021/jp211900z | J. Phys. Chem. C 2012, 116, 22266−22280

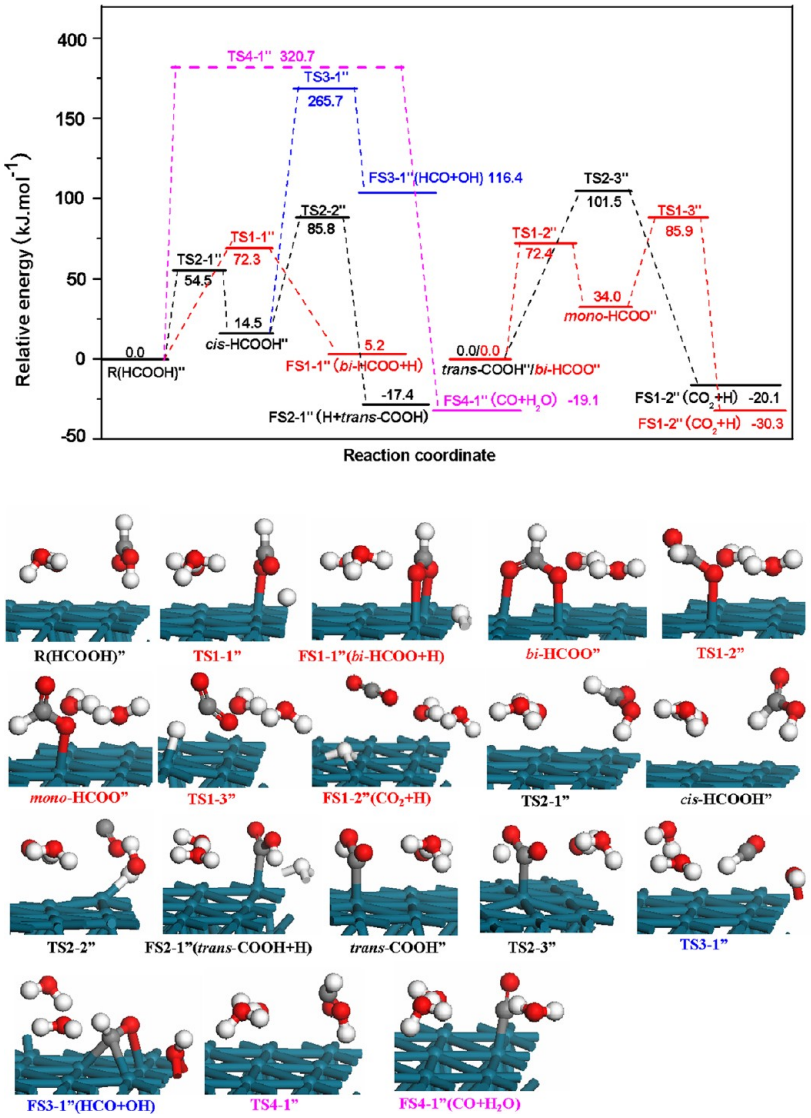

Figure 10. Potential energy profiles for HCOOH decomposition on Pd(111) surface in the presence of single adsorbed H_2O molecule, as well as the structures of the intermediates, transition states and products: TS, transition state; FS, final state. Bond lengths are in Å. See Figure 2 for color coding.

energy of 110.4 and −14.4 kJ·mol^{-1}, respectively. ***(III) The initial C−O bond cleavage and the simultaneous O−H and C−H bonds cleavage of HCOOH***: the highest barrier and reaction energy for the initial C−O bond cleavage of HCOOH are 147.3 and 69.1 kJ·mol^{-1}, respectively, whereas those for the simultaneous O−H and C−H bonds cleavage of HCOOH are 320.8 and −39.3 kJ·mol^{-1}, respectively.

Above results show that the initial C−O bond cleavage and the simultaneous O−H and C−H bonds cleavage of HCOOH is unlikely to be favorable pathway in comparison with the initial C−O and O−H bond cleavage of HCOOH on Pd(111) surface, and the reaction of HCOOH decomposition along both the O−H and C−H bond cleavage leading to CO_2 formation, via *bi*-HCOO and *trans*-COOH intermediates, respectively, should be a parallel dominant pathway due to the nearly identical highest barrier and reaction energy (+80.9 and −33.5 kJ·mol^{-1} vs +82.2 and −10.2 kJ·mol^{-1}).

(B). HCOOH Decomposition in the Presence of the Coadsorbed Two H_2O Molecules. For two H_2O molecules coadsorbed with HCOOH on Pd(111) surface, as shown in Figure 10, we can obtain the following data. ***(I) The initial O−H bond cleavage of HCOOH***: the activation barrier and reaction energy for the initial O−H bond cleavage of HCOOH are 72.3 and 5.2 kJ·mol^{-1}, respectively; meanwhile, for the formation of CO_2 with respect to *bi*-HCOO species, the highest barrier and reaction energy through a *mono*-HCOO intermediate are 85.9 and −30.3 kJ·mol^{-1}, respectively, CO_2 is formed by the routes of R(HCOOH) → *bi*-HCOO + H→*mono*-HCOO + H → CO_2 + 2H, however, the rate-determining step is changed to the C−H bond cleavage of *mono*-HCOO with the highest barrier and reaction energy of 85.9 and −30.3 kJ·mol^{-1} in comparison with that of the initial O−H bond cleavage of HCOOH in the gas phase with the highest barrier and reaction energy of 96.5 and 2.6 kJ·mol^{-1}, respectively. ***(II) The initial C−H bond cleavage of HCOOH***: the activation barrier and reaction energy for the initial C−H bond cleavage of HCOOH are +85.8 and −17.4 kJ·mol^{-1}, respectively, meanwhile, for the formation of CO_2 with respect to *trans*-COOH species, the highest barrier and reaction energy are 101.5 and −20.1 kJ·mol^{-1}, respectively. The reaction route of R(HCOOH) → *trans*-COOH + H → CO_2 +

dx.doi.org/10.1021/jp211900z | J. Phys. Chem. C 2012, 116, 22266−22280

Table 2. Activation Barrier (E_a) and Reaction Energy (ΔH) (kJ·mol^{-1}) of Elementary Reaction for the Decomposition of HCOOH on Pd(111) Surface in the Presence of the Coadsorbed Single and Two H_2O Molecules

	gas phase		single H_2O molecule		two H_2O molecule	
reactions	E_a	ΔH	E_a	ΔH	E_a	ΔH
trans-HCOOH→*bi*-HCOO + H	96.5	2.6	67.8	10.3	72.3	5.2
bi-HCOO→*mono*-HCOO + H	84.9	61.6	80.9	24.3	72.4	34.0
mono-HCOO → CO_2 + H	16.1	−89.1	49.2	−57.8	51.9	−64.3
bi-HCOO → CO_2 + H	143.0	−27.5	106.1	−33.5	116.1	−30.3
trans-HCOOH→*cis*-HCOOH	70.9	29.4	79.9	11.6	54.5	14.5
cis-HCOOH→*trans*-COOH + H	81.0	−43.8	52.5	−32.0	71.3	−31.9
trans-COOH → CO_2 + H	105.1	−21.7	82.2	−10.2	101.5	−20.1
cis-HCOOH→HCO + OH	136.1	87.9	135.7	57.5	251.2	101.9
trans-HCOOH → CO + H_2O	322.2	−81.8	320.8	−39.3	320.7	−19.1

2H is responsible for CO_2 formation, however, the O−H bond cleavage of *trans*-COOH becomes the rate-determining step with the highest barrier and reaction energy are 101.5 and −20.1 kJ·mol^{-1} in comparison with that of the initial C−H bond cleavage of HCOOH in gas phase molecule with an activation barrier and reaction energy of 110.4 and −14.4 kJ·mol^{-1}, respectively. ***(III) The initial C−O bond and the simultaneous O−H and C−H bonds cleavage of HCOOH***: the highest barrier and reaction energy of the initial step for C−O bond cleavage are 265.7 and 116.4 kJ·mol^{-1}, respectively, whereas, those for the simultaneous O−H and C−H bonds cleavage are +320.7 and −19.1 kJ·mol^{-1}, respectively.

Above results suggest that the initial C−O bond cleavage and the simultaneous O−H and C−H bonds cleavage of HCOOH is unlikely to be favorable pathway in comparison with the initial C−O and O−H bond cleavage of HCOOH on Pd(111) surface, meanwhile, the reaction of HCOOH decomposition along the O−H bond cleavage leading to CO_2 formation via *bi*-HCOO (+85.9 and −30.3 kJ·mol^{-1}) becomes more favorable both kinetically and thermodynamically in comparison with the reaction of HCOOH decomposition along the C−H bond cleavage leading to CO_2 formation via *trans*-COOH intermediates (+101.5 and −20.1 kJ·mol^{-1}), which means that CO_2 is preferentially formed via formate mechanism (via HCOO intermediates).

3.4.3. Brief Summary. On the basis of the above calculated data, we can conclude that at low coverage of 1/9 ML, the coadsorbed H_2O molecule and its coverage can slightly affect the adsorption ability of HCOOH on Pd(111) surface, however, it can obviously affect the activation barrier and reaction energy of every elementary reaction involving in the decomposition of HCOOH on Pd(111) surface. Moreover, the presence of coadsorbed H_2O can reduce the highest barrier of the initial O−H and C−H bond cleavage of HCOOH leading to CO_2, which make the reaction of HCOOH decomposition becomes more favorable both kinetically and thermodynamically in comparison with those in the gas phase. Further, the presence of coadsorbed H_2O can alter the rate-determining step of the whole HCOOH decomposition in comparison with those in the gas phase. Finally, the presence of coadsorbed H_2O can affect the dominate reaction mechanism for CO_2 formation, such as the decomposition of HCOOH goes through via the dual-path mechanism (via HCOO and COOH intermediate, respectively) of HCOOH decomposition both in the gas phase and in the presence of single adsorbed H_2O molecule, respectively, however, the decomposition of HCOOH follows the formate mechanism (via HCOO intermediate) of HCOOH decomposition in the presence of two adsorbed H_2O molecules, suggesting that the preferred catalytic pathway is qualitatively dependent on surface H_2O coverage.

On the other hand, the studies by Jacob et al.[18] has experimentally and theoretically investigated the oxidation of HCOOH on Pt(111) surface under gas-phase and coadsorbed H_2O conditions to probe the electro-catalytic HCOOH conversion in fuel cells, as well as how H_2O and its coverage affects reaction intermediate structures and transition states, their results show that HCOOH oxidation under a water-covered surface behaves substantially differently than in the gas phase or using a solvation model involving only a few water molecules, and the coadsorbed H_2O on surface plays an important role in HCOOH oxidation influencing the structure of reaction intermediates and reaction activation barriers on Pt(111) surface, as a result, the preferred catalytic pathway is also qualitatively dependent on surface coverage, the results by Jacob et al.[18] is similar to our results, suggesting that, for the decomposition reaction of HCOOH on Pd(111) and Pt(111) surfaces under a realistic condition, the effect of the coadsorbed H_2O and its coverage should be taken into account.

3.5. Comparisons with Other Metal Surfaces. Since Ni, Pd, and Pt are the 10th group elements, it is interesting to compare our calculated results about the geometric and energetic properties of Pd with previous theoretical studies of Pd by Zhou et al.,[46] Ni by Luo et al.[63] and Pt by Jacob et al.[18,64] for HCOOH adsorption and decomposition, as well as the experimental findings on Pd by Miyake et al,[65] in which the studies by Zhou et al.[46] have investigated the HCOOH adsorption and its decomposition only via C−H and O−H bond cleavage.

3.5.1. The Adsorption and Decomposition of HCOOH. On Pd(111) surface, our results show that the carbonyl O atom of HCOOH binds with Pd atom and the H atom of OH group points toward another surface Pd atoms, and HCOOH stands perpendicularly over the surface with an adsorption energy of 59.3 kJ·mol^{-1}, and the O−H bond cleavage of HCOOH has an activation barrier of 96.5 kJ·mol^{-1} and is endothermic by 2.6 kJ·mol^{-1} for the coadsorbed *bi*-HCOO and H, whereas, the activation barrier of its back reaction is 93.9 kJ·mol^{-1}. Zhou et al. have shown that HCOOH lies flat on Pd(111) surface and bonds the surface with C and O atoms with "parallel bridge" mode, which is more stable adsorption configuration with an adsorption energy of 38.6 kJ·mol^{-1} than "vertical top" mode, however, our results show this "parallel bridge" mode is less stable and converted into "vertical top" mode over the surface. Meanwhile, the O−H bond cleavage of HCOOH with "parallel bridge" mode in Zhou et al. is the favorable pathway to form HCOO species standing over the surface with only one oxygen binding to Pd−Pd bridge, this elementary reaction has an activation barrier of 20.2 kJ·mol^{-1} and is endothermic by 11.2 kJ·mol^{-1}, and the barrier of its back reaction is only 9.0

dx.doi.org/10.1021/jp211900z | J. Phys. Chem. C 2012, 116, 22266−22280

kJ·mol^{-1}, as a result, we think that HCOO can easily interact with H to form HCOOH rather than the O−H bond cleavage of HCOOH, suggesting that HCOOH with "parallel bridge" mode on Pd(111) surface in the study by Zhou et al. goes against the O−H cleavage of HCOOH. Our results show that HCOOH with "vertical top" mode on Pd(111) surface is in favor of the O−H cleavage of HCOOH leading to HCOO species standing over the surface with two oxygen binding to Pd−Pd bridge in a bidentate form. On Pt(111) surface, the studies by Jacob et al. showed that HCOOH also binds with its carbonyl O atom to an atop site and its H atom of OH group pointing down toward another adjacent atop site, and HCOOH also stands perpendicularly on the surface; the calculated adsorption energy is 38.6 kJ·mol^{-1}; the activation barrier of O−H bond cleavage is found to be endothermic by 1.9 kJ·mol^{-1} with an activation barrier of 90.7 kJ·mol^{-1} at 1/9 ML. On Ni(111) surface, similar to HCOOH adsorbed on Pd(111) and Pt(111) surfaces, the carbonyl O atom of HCOOH still binds with an atop Ni atom, and its H atom of OH group points toward another adjacent surface Ni atom. HCOOH stands perpendicularly over the surface with an adsorption energy of 34.7 kJ·mol^{-1}. The activation barrier of the O−H bond cleavage leading to the coadsorbed HCOO and H is 39.6 kJ·mol^{-1} and is exothermic by 33.8 kJ·mol^{-1}.

On the basis of above comparisons, we can see that at 1/9 ML coverage, HCOOH standing perpendicularly over the Pd, Pt, and Ni(111) surfaces is the most stable configurations with its carbonyl O atom binding with atop atom. The adsorption energy of HCOOH on Pd, Pt, and Ni(111) surfaces is 59.3, 38.6, and 34.7 kJ·mol^{-1}, respectively. The corresponding activation barrier of O−H bond cleavage is 96.5, 90.7, and 39.6 kJ·mol^{-1}, respectively. These results indicate that HCOOH adsorbed on Pd has the most stable configuration and the highest activation barrier of the O−H bond cleavage among three metal surfaces.

In addition, Jorgensen and Madix[66] have investigated the reactions of HCOOH on the clean and oxygen-predosed Pd(100) surface by using temperature-programmed reaction and vibrational spectroscopy, suggesting that on the clean Pd(100) surface, HCOOH can partially decomposes to give CO, however, the HCOO species was identified on the oxygen-precovered surface. Sander and Erley[67] have experimentally investigated the decomposition of HCOOH on Pd(100), the infrared spectroscopy and TDS results show that under the thermal decomposition of HCOOH on Pd(100) at a temperature as low as 170 K, one of the decomposition reaction pathways seems to produce directly adsorbed CO, hydrogen, and oxygen. Furthermore, Aas et al.[68] have studied the adsorption and decomposition of HCOOH on Pd(110) surface, which show that the HCOOH molecules on Pd are not stable, but are decomposed and desorbed as H_2, CO, CO_2, and H_2O, and the evolution of CO_2 derive from the intermediate HCOO. These studies suggest that different crystal surface of Pd may show different catalytic behavior for HCOOH decomposition leading to different dominant products.

3.5.2. The Adsorption and Decomposition of HCOO. On Pd(111) surface, the experimental findings by Miyake et al.[65] propose that HCOO is a short-lived reactive intermediate in the case of HCOOH electro-oxidation on Pd by using surface-enhanced infrared adsorption spectroscopy in the attenuated total reflection mode (ATR-SEIRAS). The studies by Zhou et al. show that HCOO species binds the Pd(111) surface in a bidentate form is the most stable adsorption configuration with an adsorption energy of 49.2 kJ·mol^{-1}, our results show that HCOO species in a bidentate form over Pd(111) surface is also the most stable adsorption configuration; however, the adsorption energy is 260.3 kJ·mol^{-1}. Similarly, on Ni(111) and Pt(111) surfaces at 1/9 ML, HCOO species adsorbed on the surface in a bidentate form is also the most stable configuration. The adsorption ability of HCOO in a bidentate form on metal surfaces is in the order of Ni (273.1 kJ·mol^{-1}) > Pd (260.3 kJ·mol^{-1}) > Pt (223.9 kJ·mol^{-1}); Further, the decomposition of HCOO in a bidentate form on Pd(111), Ni(111), and Pt(111) surfaces, leading to CO_2 and H, all goes through a relatively unstable intermediate HCOO in monodentate form; the corresponding effective activation barrier on Pd(111), Ni(111), and Pt(111) surfaces is 84.9, 99.4, and 150.5 kJ·mol^{-1}, respectively. Taking into consideration the activation barrier of O−H bond cleavage of HCOOH, we can conclude that Pd has the lowest effective activation barrier for HCOO decomposition (96.5 kJ·mol^{-1}), followed by Ni (99.4 kJ·mol^{-1}) and Pd (150.5 kJ·mol^{-1}), suggesting that Pd is the most suitable metal to catalyze the decomposition of HCOOH.

4. CONCLUSIONS

In this study, four possible pathways of HCOOH decomposition on Pd(111) surface, initiated by the activation of the C−H, O−H, and C−O bonds of HCOOH, as well as the activation of simultaneous C−H and C−O bonds, have been proposed and discussed to identify the preference of CO_2 or CO as the dominant product by using periodic, self-consistent density functional theory calculations. Then, the effects of coadsorbed H_2O and its coverage on the decomposition of HCOOH have been also discussed in details. Our results show that CO_2 is preferentially formed as the dominant product of HCOOH decomposition on Pd(111) surface. The formation of CO_2 is initiated by the O−H and C−H bond cleavage of HCOOH, in which both the carboxyl (*trans*-COOH) and formate (*bi*-HCOO) reactive intermediates are involved, along with alternative bond-breaking possible steps in those intermediates. The sequence dehydrogenation of HCOOH on the Pd surface is a vital process for CO_2 formation, and the presence of coadsorbed H_2O can alter the rate-determining step and reaction mechanism of the whole HCOOH decomposition in comparison with those in the gas phase, suggesting that the preferred catalytic pathway is qualitatively dependent on surface H_2O coverage. Our results would at the microscopic level provide insights into the mechanism, energetics, and possible reactive intermediates of HCOOH decomposition regarding the preference of CO_2 formation as the dominant product for catalytic reactions involving HCOOH and for direct HCOOH fuel cells on Pd system.

AUTHOR INFORMATION

Corresponding Author

*No. 79 Yingze West Street, Taiyuan 030024, China. Telephone: +86 351 6018539. Fax: +86 351 6041237 E-mail address: wangbaojun@tyut.edu.cn or quantumtyut@126.com.

Notes

The authors declare no competing financial interest.

ACKNOWLEDGMENTS

This works is financially supported the National Natural Science Foundation of China (20906066, 21276003, and

20976115). The authors thank for anonymous reviewers for their helpful suggestions on the quality improvement of our present paper.

REFERENCES

(1) Zhu, Y.; Ha., S.; Masel, R. I. *J. Power Sources* **2004**, *130*, 8−14.
(2) Zhu, Y.; Khan, Z.; Masel, R. I. *J. Power Sources* **2005**, *139*, 15−20.
(3) Lin, Z. L.; Hong, L.; Tham, M. P.; Lim, T. H.; Jiang, H. X. *J. Power Sources* **2006**, *161*, 831−835.
(4) Larsen, R.; Ha, S.; Zakzeski, J.; Masel, R. I. *J. Power Sources* **2006**, *157*, 78−84.
(5) Yu, X. W.; Pickup, P. G. *J. Power Sources* **2008**, *182*, 124−132.
(6) Tedsree, K.; Li, T.; Jones, S.; Chan, C. W. A.; Yu, K. M. K.; Bagot, P. A. J.; Marquis, E. A.; Smith, G. D. W.; Tsang, S. C. E. *Nat. Nano.* **2011**, *6*, 302−307.
(7) Wang, J. Y.; Kang, Y. Y.; Yang, H.; Cai, W. B. *J. Phys. Chem. C* **2009**, *113*, 8366−8372.
(8) Uhm, S.; Lee, H. J.; Kwon, Y.; Lee, J. *Angew. Chem., Int. Ed.* **2008**, *47*, 10163−10166.
(9) Zhang, H. X.; Wang, C.; Wang, J. Y.; Zhai, J. J.; Cai, W. B. *J. Phys. Chem. C* **2010**, *114*, 6446−6451.
(10) Wang, J. Y.; Zhang, H. X.; Jiang, K.; Cai, W. B. *J. Am. Chem. Soc.* **2011**, *133*, 14876−14879.
(11) Ha, S.; Larsen, R.; Masel, R. I. *J. Power Sources* **2005**, *144*, 28−34.
(12) Miesse, C. M.; Jung, W. S.; Jeong, K. J.; Lee, J. K.; Lee, J. Y.; Han, J. H.; Yoon, S. P.; Nam, S. W.; Lim, T. H.; Hong, S. A. *J. Power Sources* **2006**, *162*, 532−540.
(13) Clarence, M. Y. Y.; Lim, K. H. *Catal. Lett.* **2009**, *128*, 221−226.
(14) Jacobs, G.; Patterson, P. M.; Graham, U. M.; Crawford, A. C.; Davis, B. H. *Int. J. Hydrogen Energy* **2005**, *30*, 1265−1276.
(15) Feliu, J. M.; Herrero, E. In *Handbook of Fuel Cells*Vielstich, W., Gasteiger, H. A., Lamm, A., Eds.; Wiley: New York, 2003; Vol. 2, p 679.
(16) Chen, A. C.; Holt-Hindle, P. *Chem. Rev.* **2010**, *110*, 3767−3804.
(17) Macia, M. D.; Herrero, E.; Feliu, J. M.; Aldaz, A. *J. Electroanal. Chem.* **2001**, *500*, 498−509.
(18) Gao, W.; Keith, J. A.; Anton, J.; Jacob, T. *J. Am. Chem. Soc.* **2010**, *132*, 18377−18385.
(19) Wilhelm, S.; Vielstich, W.; Buschmann, H.; Iwasita, T. *J. Electroanal. Chem.* **1987**, *229*, 377−384.
(20) Capon, A.; Parsons, R. *J. Electroanal. Chem.* **1973**, *45*, 205−231.
(21) Sun, S.; Clavilier, J.; Bewick, A. *J. Electroanal. Chem.* **1988**, *240*, 147−159.
(22) Samjeské, G.; Osawa, M. *Angew. Chem., Int. Ed.* **2005**, *44*, 5694−5698.
(23) Samjeské, G.; Miki, A.; Ye, S.; Yamakata, A.; Mukouyama, Y.; Okamoto, H.; Osawa, M. *J. Phys. Chem. B* **2005**, *109*, 23509−23516.
(24) Mukouyama, Y.; Kikuchi, M.; Samjeské, G.; Osawa, M.; Okamoto, H. *J. Phys. Chem. B* **2006**, *110*, 11912−11917.
(25) Zhang, R. G.; Wang, B. J.; Liu, H. Y.; Ling, L. X. *J. Phys. Chem. C* **2011**, *115*, 19811−19818.
(26) Zhang, R. G.; Liu, H. Y.; Wang, B. J.; Ling, L. X. *Appl. Catal. B; Environ.* **2012**, *126*, 108−120.
(27) Pan, Y. X.; Liu, C. J.; Ge, Q. F. *J. Catal.* **2010**, *272*, 227−234.
(28) Zhang, R. G.; Song, L. Z.; Wang, B. J.; Li, Z. *J. Comput. Chem.* **2012**, *33*, 1101−1110.
(29) Huo, C. F.; Li, Y. W.; Wang, J. G.; Jiao, H. J. *J. Am. Chem. Soc.* **2009**, *131*, 14713−14721.
(30) Liu, Z. P.; Hu, P. *J. Am. Chem. Soc.* **2003**, *125*, 1958−1967.
(31) Chin, Y. H.; Buda, C.; Neurock, M.; Iglesia, E. *J. Catal.* **2011**, *283*, 10−24.
(32) Mei, D. H.; Neurock, M.; Smith, C. M. *J. Catal.* **2009**, *268*, 181−195.
(33) Carr, R. T.; Neurock, M.; Iglesia, E. *J. Catal.* **2011**, *278*, 78−93.
(34) Lin, C. H.; Chen, C. L.; Wang, J. H. *J. Phys. Chem. C* **2011**, *115*, 18582−18588.
(35) Cheng, J.; Gong, X. Q.; Hua, P.; Lok, C. M.; Ellis, P.; French, S. *J. Catal.* **2008**, *254*, 285−295.
(36) Hammer, B.; Norskov, J. K. *Adv. Catal.* **2000**, *45*, 71−129.
(37) Norskov, J. K.; Bligaard, T.; Hvolbak, B.; Abild-Pedersen, F.; Chorkendorff, I.; Christensen, C. H. *Chem. Soc. Rev.* **2008**, *37*, 2163−2171.
(38) Delley, B. *J. Chem. Phys.* **1990**, *92*, 508−517.
(39) Delley, B. *J. Chem. Phys.* **2000**, *113*, 7756−7764.
(40) Perdew, J. P.; Wang, Y. *Phys. Rev. B* **1992**, *45*, 13244−13249.
(41) Hohenberg, P.; Kohn, W. *Phys. Rev. B* **1964**, *136*, B864−B871.
(42) Dolg, M.; Wedig, U.; Stoll, H.; Preuss, H. *J. Chem. Phys.* **1987**, *86*, 866−872.
(43) Bergner, A.; Dolg, M.; Kuechle, W.; Stoll, H.; Preuss, H. *Mol. Phys.* **1993**, *80*, 1431−1441.
(44) Halgren, T. A.; Lipscomb, W. N. *Chem. Phys. Lett.* **1977**, *49*, 225−232.
(45) Holtzberg, F.; Post, B.; Fankuchen, I. *Acta Crystallogr.* **1953**, *6*, 127−130.
(46) Zhou, S. D.; Qian, C.; Chen, X. Z. *Catal. Lett.* **2011**, *141*, 726−734.
(47) Wang, G. C.; Morikawa, Y.; Matsumoto, T.; Nakamura, J. *J. Phys. Chem. B* **2006**, *110*, 9−11.
(48) Lim, K. H.; Moskaleva, L. V.; Rösch, N. *Chem. Phys. Chem.* **2006**, *7*, 1802−1812.
(49) Sautet, P.; Rose, M. K.; Dunphy, J. C.; Behler, S.; Salmeron, M. *Surf. Sci.* **2000**, *453*, 25−31.
(50) Chen, Z. X.; Neyman, K. M.; Lim, K. H.; Rösch, N. *Langmuir* **2004**, *20*, 8068−8077.
(51) Lim, K. H.; Chen, Z. X.; Neyman, K. M.; Rösch, N. *J. Phys. Chem. B* **2006**, *110*, 14890−14897.
(52) Felter, T. E.; Sowa, E. C. *Phys. Rev. B* **1989**, *40*, 891−899.
(53) Yudanov, I. V.; Neyman, K. M.; Rösch, N. *Phys. Chem. Chem. Phys.* **2004**, *6*, 116−123.
(54) Dong, W.; Ledentu, V.; Sautet, P.; Eichler, A.; Hafner, J. *Surf. Sci.* **1998**, *411*, 123−136 and references therein..
(55) Shustorovich, E. *Adv. Catal.* **1990**, *37*, 101−163.
(56) Columbia, M. R.; Thiel, P. A. *J. Electroanal. Chem.* **1994**, *369*, 1−14.
(57) Woodruff, D. P.; McConville, C. F.; Kilcoyne, A. L. D.; Linder, Th.; Somers, J.; Surman, M.; Paolucci, G.; Bradshaw, A. M. *Surf. Sci.* **1988**, *201*, 228−244.
(58) Wander, A.; Holland, B. W. *Surf. Sci.* **1988**, *199*, L403−L405.
(59) Casarin, M.; Granozzi, G.; Sambi, M.; Tondello, E.; Vittadini, A. *Surf. Sci.* **1994**, *307*, 95−100.
(60) Mehandru, S. P.; Anderson, A. B. *Surf. Sci.* **1989**, *219*, 68−76.
(61) Holdcroft, S.; Lionel Funt, B. *J. Electroanal. Chem.* **1988**, *240*, 89−103.
(62) Mehmood, F.; Greeley, J.; Curtiss, L. A. *J. Phys. Chem. C* **2009**, *113*, 21789−21796.
(63) Luo, Q.; Feng, G.; Beller, M.; Jiao, H. *J. Phys. Chem. C* **2012**, *116*, 4149−4156.
(64) Gao, W.; Keith, J. A.; Anton, J.; Jacob, T. *Dalton Trans.* **2010**, *39*, 8450−8456.
(65) Miyake, H.; Okada, T.; Samjeské, G.; Osawa, M. *Phys. Chem. Chem. Phys.* **2008**, *10*, 3662−3669.
(66) Jorgensen, S. W.; Madix, R. J. *J. Am. Chem. Soc.* **1988**, *110*, 397−400.
(67) Sander, D.; Erley, W. *J. Vac. Sci. Technol. A* **1990**, *8*, 3357−3359.
(68) Aas, N.; Li, Y.; Bowker, M. *J. Phys.: Condens. Matter* **1991**, *3*, S281−S286.